

1 The Liquid Argon Purity Demonstrator

2 M. Adamowski^a, B. Carls^a, E. Dvorak^b, A. Hahn^a, W. Jaskierny^a, C. Johnson^a, H. Jostlein^a,
3 C. Kendziora^a, S. Lockwitz^a, B. Pahlka^{a*}, R. Plunkett^a, S. Pordes^a, B. Rebel^a, R. Schmitt^a,
4 M. Stancari^a, T. Tope^{a†}, T. Yang^a

5 ^aFermi National Accelerator Laboratory, P.O. Box 500, Batavia, IL, 60510, USA

6 ^bSouth Dakota School of Mines & Technology, 501 East Saint Joseph Street, Rapid City, SD
7 57701

8 **ABSTRACT**

9 The Liquid Argon Purity Demonstrator was a project to determine if electron drift lifetimes
10 adequate for large neutrino detectors could be achieved in a commercial cryostat without evac-
11 uation. We describe here the cryogenic system, the operations used to achieve multi-millisecond
12 electron drift-lifetimes, the apparatus used to determine the contaminant levels in the argon and
13 to measure the electron drift lifetime, and report on the results obtained. Measurements of the
14 temperature profile in the argon were also made and are compared to simulation.

15 **1. Introduction**

16 Liquid argon (LAr) time projection chambers (TPCs) provide a robust and elegant method
17 for measuring the properties of neutrino interactions above a few hundred MeV by providing 3D
18 event imaging with excellent spatial resolution. The ionization electrons created by the passage
19 of charged particles through the liquid can be transported with typical diffusion of less than
20 a mm by a uniform electric field over macroscopic distances. Imaging is achieved by sets of
21 parallel wires oriented in different directions and perpendicular to the drift field. The signals
22 induced by the drifting electrons on the wires are amplified and digitized by wave-form recording
23 electronics. The projection of a particle track in the plane perpendicular to the drift field, i.e.
24 the plane of the wires, is given by the pattern of hits on the wire planes while the projection
25 of the track in the plane perpendicular to the wires is given by the arrival time of the signals
26 on the wires [1,2]. This technology requires that electrons drift without becoming attached to
27 electronegative contaminants. LArTPC technology has experienced renewed and strengthened
28 interest since having recently been chosen as the preferred technology for the LBNE future
29 long-baseline neutrino oscillation experiment [3].

30 The ICARUS Collaboration led a pioneering effort in the research and development of LAr
31 TPC technology culminating in the construction of the T600 LArTPC in 2001 [5]. The T600
32 LArTPC is housed in a 760 ton cryostat which is surrounded by insulating layers of Nomex
33 honeycomb cells [4]. Before filling the cryostat with liquid argon, the inner surfaces were baked
34 until a pressure of 10^{-4} mbar inside the evacuated cryostat was achieved. Electron lifetimes
35 greater than 6 ms were obtained with a contamination less than 50 parts per trillion (ppt)
36 oxygen equivalent.

*Corresponding author: pahlka@fnal.gov (B. Pahlka)

†Corresponding author: tope@fnal.gov (T. Tope)

1 The Materials Test Stand (MTS) at the Fermi National Accelerator Laboratory (Fermilab)
 2 was developed to evaluate the effect of different materials on electron lifetime [6]. The system
 3 uses a 250 L vacuum-insulated vessel that was evacuated to a pressure of 10^{-6} Torr before filling.
 4 The system employed commercial argon filters to reduce contamination from water and oxygen
 5 and measured electron lifetimes of approximately 8 ms using a dedicated purity monitor.

6 The ArgoNeuT project at Fermilab was the first LArTPC in The United States to be placed
 7 in a neutrino beam [8]. Commissioned in 2009, it had an 550 L vacuum insulated cryostat that
 8 was evacuated before filling with LAr. The purification system only purified reliquefied argon
 9 gas boiled-off in the gaseous region of the cryostat. With this system, ArgoNeuT was able to
 10 obtain lifetimes of about 750 μ s.

11 The ARGONTUBE LArTPC of AEC-LHEP University of Bern was developed to investigate
 12 the ability to drift electrons over distances of up to 5 m [9]. It uses a vacuum insulated cryostat
 13 and is evacuated to 5×10^{-5} mbar before filling with LAr. ARGONTUBE has been able to
 14 reach contamination levels down to 1 part per million (ppm)(really?) and achieve lifetimes of 2
 15 ms with a 240 V/cm drift field **check with T. Strauss**.

16 The conventional liquid argon vessels described in this section were evacuated to remove water,
 17 oxygen, and nitrogen contaminants present in the ambient air prior to filling with liquid argon.
 18 However, physics requirements for long-baseline neutrino experiments dictate larger cryogenic
 19 vessels to hold bigger detectors and the mechanical strength required to resist the external
 20 pressure of evacuation becomes prohibitively costly. Thus, the concept of purification without
 21 evacuation and testing with LAPD was proposed in 2006 [23].

22 The Liquid Argon Purity Demonstrator (LAPD) located at Fermilab was designed to achieve
 23 the ultra high purity required by LArTPCs in a vessel that cannot be evacuated. The system
 24 relies heavily on the experience from the MTS [6] in its design and operation plan. Argon
 25 purification proceeded in three stages. Electron lifetimes on the order of several milliseconds are
 26 achieved through a sequence of steps as follows. Previous studies suggest that the concentration
 27 of oxygen in a vessel purged with gaseous argon can be reduced to 100 ppm after 2.6 volume
 28 exchanges [7]. Thus, prior to filling with liquid argon, ambient air in the cryostat is removed
 29 by purging the tank with argon gas. After the initial purge, the walls of the cryostat are
 30 heated to dry the surfaces of the vessel. Once the water and oxygen concentrations are at the
 31 level of a few parts per million (ppm), the gas is subsequently circulated through filter vessels to
 32 further reduce these contaminants. Liquid argon is then introduced into the vessel after impurity
 33 concentrations less than 1 ppm are achieved. The liquid is then continuously circulated through
 34 the filter vessels in order to achieve concentrations of water and oxygen on the order of 0.1 parts
 35 per billion (ppb). A photograph of the LAPD vessel is shown in Figure 1.

36 The LAPD had several secondary goals. First, we studied the number of liquid argon volume
 37 exchanges necessary to achieve drift distances on the scale of 2.5 meters. Second, we compared
 38 simulations of liquid argon temperature gradients and impurity concentrations in the cryostat to
 39 our measurements using dedicated instruments installed in the cryostat. Third, we monitored
 40 and evaluated filter capacity performance as a function of flow rate. Finally, after achieving
 41 the required electron drift lifetimes, the LAPD cryostat was emptied and a TPC of 2 m drift
 42 distance was installed in the central cryostat region. High liquid argon purity was achieved with
 43 the TPC in the tank and the details of these results will be presented in a forthcoming paper.

44 2. The Cryostat

45 The LAPD cryostat is an industrial low pressure storage tank. The cryostat has a flat bottom,
 46 cylindrical sides, and a dished head. The cryostat diameter is 10 feet and the cylindrical walls

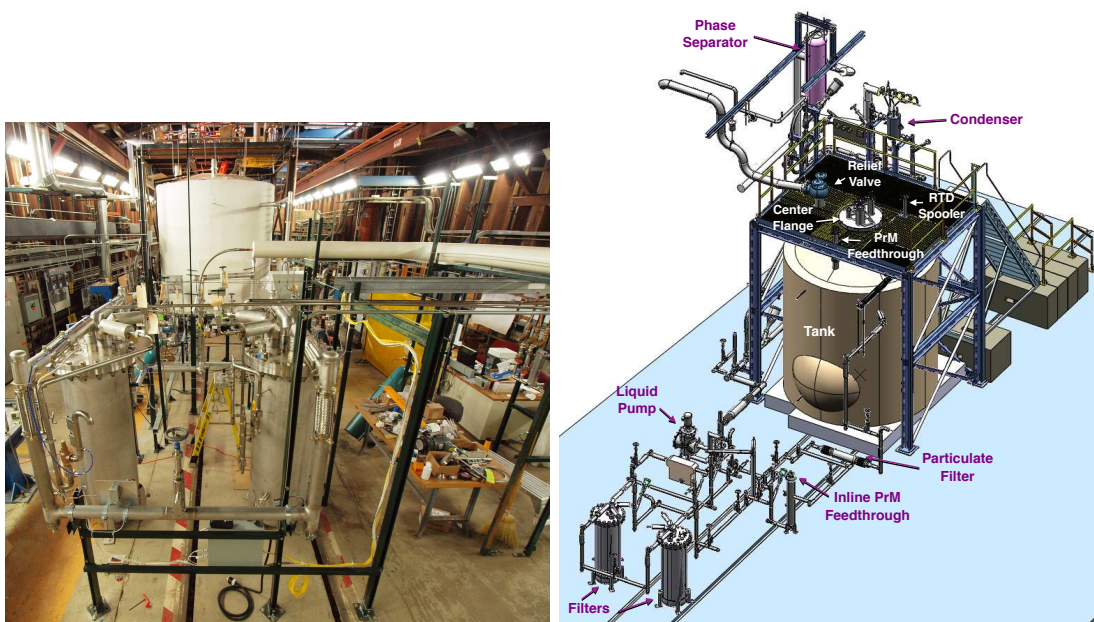


Figure 1. A photograph of the Liquid Argon Purity Demonstration (LAPD) at Fermilab (left) and 3D model of the system (right).

1 have a 10-foot height. The cryostat is fabricated from 3/16 inch-thick SA-240 stainless steel.
 2 The internal and external (vacuum) maximum allowable working pressures are 3 psig and 0.2
 3 psig, respectively. Eight perimeter anchors tie the cryostat bottom to the ground to prevent
 4 cryostat uplift. The cryostat volume is 24628 liters of which 21210 liters is liquid (29.7 tons) with
 5 a corresponding liquid depth of 2.9 m. Fabrication followed The American Petroleum Institute
 6 Standard 620 Appendix Q as closely as possible and the cryostat welds were fully radiographed.
 7 The cryostat is located inside the Proton Center 4 (PC4) building at Fermilab. Figure 2 shows
 8 a picture of the LAPD cryostat.

9 The head of the cryostat is populated with four ConFlat flanges and a 30 inch diameter
 10 center flange sealed with an indium wire. Metallic seals are used to prevent the diffusion of
 11 contamination that would occur through non-metallic seals. The center flange allows for cryostat
 12 entry using an extension ladder. Five ConFlat flanges populate the center flange, each of which
 13 sit atop stainless steel tube risers such that the ConFlats remain at room temperature when
 14 the cryostat is cold. Figure 3 shows the top of the cryostat layout. At ground level a 30 inch
 15 diameter welded manhole is available and intended to make access easier for extended work
 16 inside the cryostat. Table 1 lists the cryostat operating parameters including the heat leak,
 17 volume, operating pressure, and nominal pump flow rates.

18 The cryostat sides and top are insulated with 10 inches of fiberglass which is covered by an
 19 outer layer of 3/4 inch-thick-foam. The foam is covered with glass cloth and a layer of mastic
 20 which provides a vapor barrier. The cryostat sits on an insulating structural foam base also
 21 sealed with a mastic vapor barrier. The cryostat heat leak was estimated as 2103 W ($X W/m^3$).
 22 Natural air flow under the rail cars and cribbing eliminates the need for foundation heaters.

23 The cryostat was cleaned with deionized water and detergent then dried with lint free rags



Figure 2. LAPD cryostat sitting on an insulating foam base in PC4. Insulating foam was added to the sides and head later.

Cryostat heat leak	2100 W
Internal max. pressure	3 psig
External max. pressure	0.2 psig
Cryostat volume	24628 liters
Liquid argon volume	21210 liters
Depth at full capacity	2.9 m
Condenser cooling capacity	8400 W

Table 1

The nominal operating parameters for the LAPD including the heat leak, operating pressures, cryostat volume, and condenser cooling capacity.

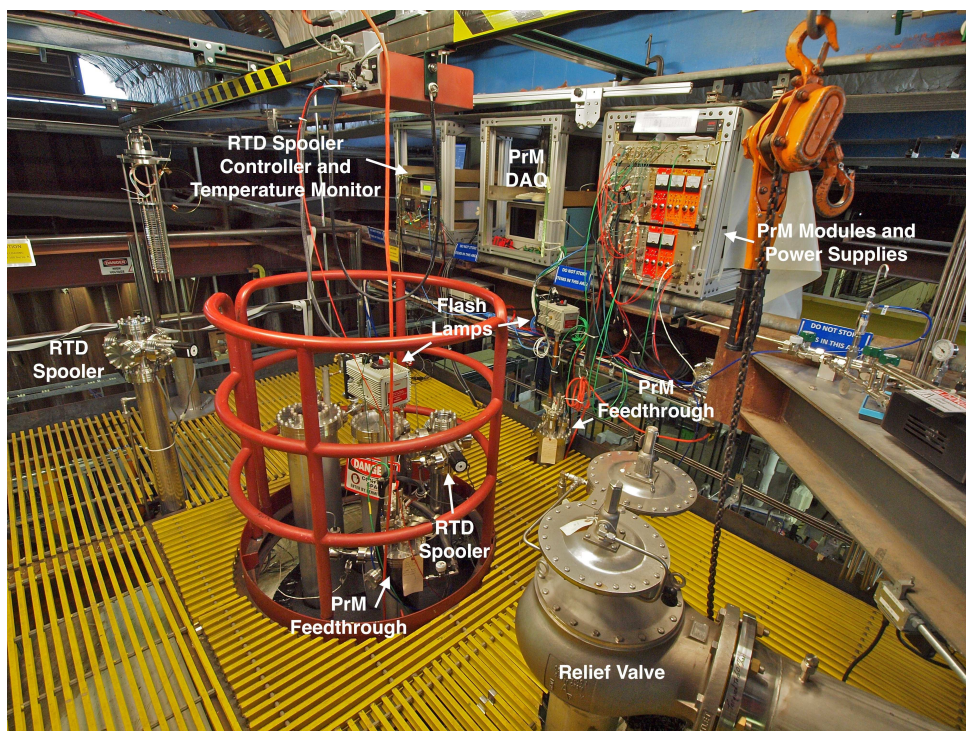


Figure 3. A photograph of the platform on top of the cryostat showing the control systems (see Section 3.5), the RTD translators (see Section 4.1), and the purity monitor feedthroughs (see Section 4.2).

1 by the cryostat fabricator prior to shipment to Fermilab. After installation of all components
2 at Fermilab, the cryostat was vacuumed with a HEPA filter equipped vacuum. After vacuum
3 cleaning, all walls were wiped with deionized water and lint free rags.

4 **3. The Cryogenics**

5 **3.1. Phase Separator and Condenser**

6 The argon vapor generated by ambient heat input is condensed using liquid nitrogen. A 4,000
7 gallon trailer supplies liquid nitrogen through foam-insulated 1 inch Type K copper piping. A
8 phase separator operating at 15 psig near the LAPD cryostat vents nitrogen vapor generated
9 in the nitrogen transfer line so that the condenser is supplied with single phase liquid nitrogen.
10 The phase separator and condenser were designed at Fermilab. A control valve feeding the phase
11 separator maintains a constant liquid level in the phase separator. The condenser consists of
12 an argon volume containing three differently sized coils of tubing through which liquid nitrogen
13 flows. The coiled nitrogen tubing is seamless and all nitrogen connections and welds are outside
14 the condenser to mitigate any nitrogen leak into the LAPD cryostat. Argon vapor is condensed
15 by the liquid nitrogen flowing through the coils.

16 Water outgassing from the tank walls, devices, and cables above the liquid is mixed with argon
17 vapor which needs to be removed to maintain high LAr purity. Thus, by default the condensed
18 liquid argon returns to the liquid recirculation pump suction before going through the filters
19 during liquid recirculation. When the pump is off, the condensed liquid argon returns directly
20 to the tank. A control valve feeds the condenser and adjusts the flow to maintain a constant
21 vapor pressure in the ullage. Solenoid valves choose which combination of coils receives liquid
22 nitrogen. The coils operate at near ambient pressure due to the pressure drop across the inlet
23 control valve. The coils will therefore be covered in a thin layer of argon ice due to the large
24 temperature gradient. Argon ice formation was accounted for in the condenser design and no
25 noticeable impact on the cooling due to the argon ice was observed. Vaporized nitrogen is vented
26 outside the enclosure and not recovered. Figure 4 shows a sketch of the condenser design and
27 Figure 5 shows a photo of the phase separator and condenser in PC4.

28 **3.2. Filters**

29 The purification system contains two filters which have identically sized filtration beds of 77
30 liters. The first filter that the process stream enters contains a 4A molecular sieve supplied
31 by Sigma-Aldrich [10] which primarily removes water contamination but can also remove small
32 amounts of nitrogen and oxygen. The second filter contains BASF CU-0226 S, a highly dispersed
33 copper oxide impregnated on a high surface area alumina to remove oxygen [11] and to a lesser
34 extent, water. Thus, the oxygen filter is placed downstream of the molecular sieve to maximize
35 oxygen filtration. The filters are insulated with vacuum jackets and aluminum radiation shields.
36 Metallic radiation shields were chosen because the filter regeneration temperatures would damage
37 traditional aluminized mylar insulation. Piping supplying the filter regeneration gas is insulated
38 both inside the filter vacuum insulation space and outside the filter with Pyrogel XT which is
39 an aerogel based insulation [12] which can withstand temperatures up to 1200 F. Figure 6 shows
40 a 3D rendering of the filter vessel.

41 The filters are regenerated in place using heated gas, which differs from the procedure per-
42 formed by ICARUS. Both filters are regenerated using a flow of argon gas heated to 200 C,
43 supplied by commercial 180 liter liquid argon dewars. Once at 200 C, a small flow of hydrogen is
44 mixed into the primary argon flow which exothermically combines with oxygen captured by the
45 filter to create water. Too much hydrogen induces temperatures which are sufficiently high to
46 damage the filter. The damage is induced by sintering of the copper which reduces the available

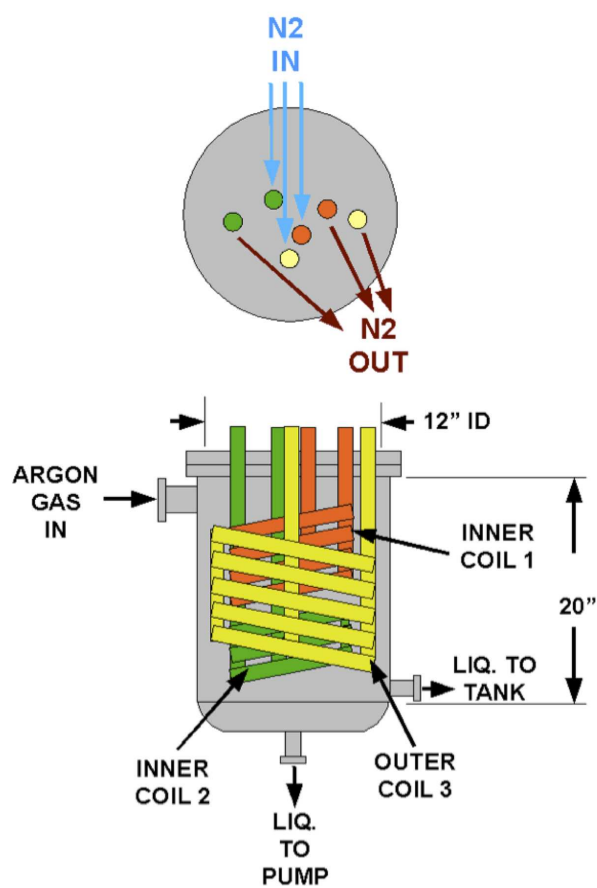


Figure 4. A sketch of the LAPD condenser which shows the three coils of tubing for liquid nitrogen, the inlet for gaseous argon and two outlets for liquefied argon.

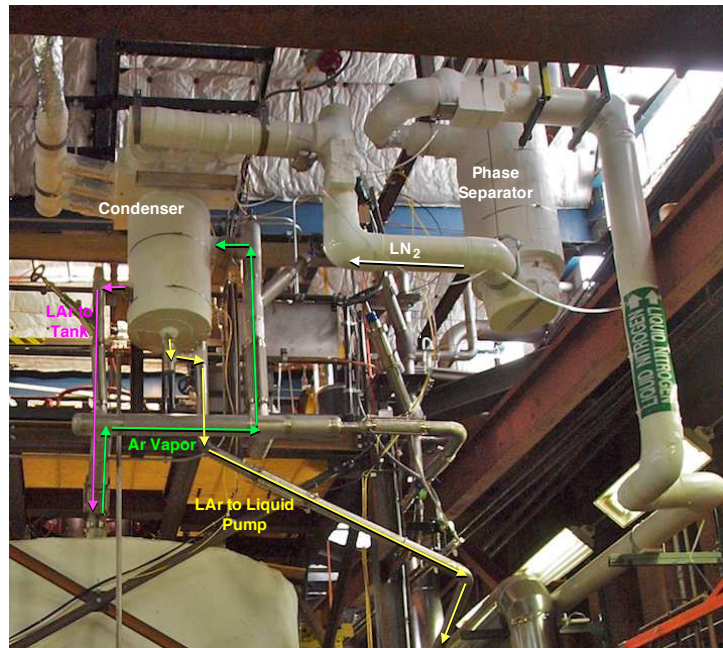


Figure 5. A photograph of the LAPD phase separator and condenser. The argon vapor path to the condenser and the two liquefied argon return paths are shown.

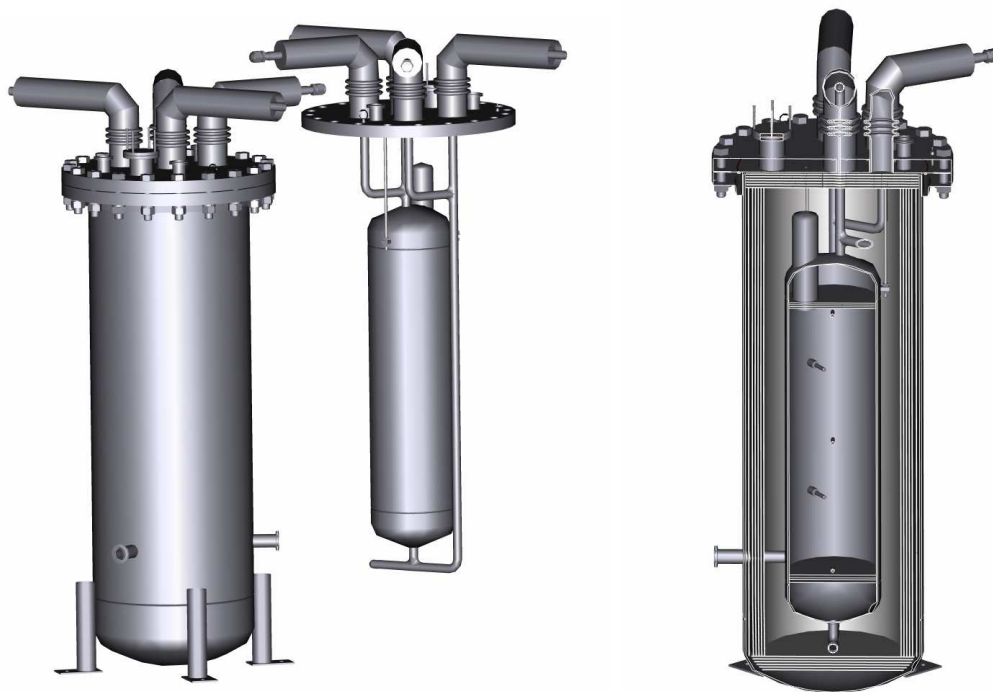


Figure 6. A 3D rendering of the filter vessel. The evacuation vessel and the canister holding the filter material are shown on the left. The cross section of the vessel is shown on the right.

1 filter surface area. Thus, precautions are taken to maintain a hydrogen fraction below 2.5% of
2 the heated gas mixture. During the heated gas regeneration, five filter bed temperature sensors
3 monitor the filter material temperature and the water content of the regeneration exhaust gas
4 is measured. Both filters are evacuated using turbomolecular vacuum pumps while they cool to
5 remove remaining trace amounts of water.

6 At the filtered liquid return to the tank, a particulate filter with an effective filtration of 10
7 microns protects the tank from any debris in the piping. The filter consists of a commercial
8 stainless steel sintered metal cylinder mounted in a custom cryogenic housing and vacuum jacket.
9 Filtration is accomplished by flowing liquid argon to the interior, then outward through the walls,
10 of the sintered metal cylinder. Flanges on the argon piping, along with flanges and edge welded
11 bellows on the vacuum jacket, allow removal of the particulate filter.

12 3.3. Piping and Valves

13 The Schedule 10 stainless steel purification piping that supplies argon to the filters is vacuum
14 jacketed. The inner line containing argon is 1 inch in diameter with a 3 inch diameter vacuum
15 jacket, except at the pump suction where the inner line is 2 inches in diameter with a 5 inch
16 diameter vacuum jacket. During the fabrication process, all piping was washed with deionized
17 water and detergent to remove oil and grease then cleaned with isopropyl alcohol. All valves as-
18 sociated with the argon purification piping utilize a metal seal with respect to ambient air either
19 through a bellows or a diaphragm to prevent the diffusion of oxygen and water contamination.
20 The exhaust side of all relief valves are continuously purged with argon gas to prevent diffusion
21 of oxygen and water from ambient air across the o-ring seal. Where possible, ConFlat flanges
22 with copper seals are used on both cryogenic and room temperature argon piping. Pipe flanges
23 in the system are sealed using spiral wound graphite gaskets (reference a part number). Smaller
24 connections are made with VCR fittings with stainless steel gaskets.

25 3.4. Recirculation Pump

26 The liquid argon pump is a Barber-Nichols [13] BNCP-32B-000 magnetically driven partial
27 emission centrifugal pump which isolates the pump and liquid argon from the electric motor. The
28 impeller, inducer, and driving section of the magnetic coupling each have their own bearings
29 which are lubricated by the liquid argon at the impeller end. The motor is controlled by a
30 variable frequency drive (VFD) which allows adjustment of the pump speed to produce the
31 desired head and flow within the available power range of the motor.

32 The liquid argon flow rate is measured at the pump discharge by an Emerson Process Man-
33 agement Micro Motion Coriolis flow meter [14]. This flow meter is appropriate for ultra high
34 purity liquid argon because, from the perspective of the liquid argon, it only consists of stainless
35 steel pipe and flanges. The inertial effects of the fluid flow through the flow meter pipes is di-
36 rectly proportional to the mass flow of the liquid. The mass flow rate is computed by measuring
37 the difference in the phase vibration between the two ends of the flow pipe. The flow curve
38 of the liquid argon pump with respect to mass flow and pressure is relatively flat, such that
39 pump speed and differential pressure are not good indicators of the mass flow rate. **Can we use**
40 **the manufacturer's plot with a proper reference?** Thus the liquid argon flowmeter is essential
41 instrumentation if the rate of filtration is to be known.

42 3.5. Control System

43 The LAPD cryogenic system is controlled by a Siemens Programmable Logic Controller (PLC).
44 The PLC reads out the pressure, liquid level, temperature, gas analyzer instrumentation, and
45 electron lifetime measured by purity monitors. Human-machine interface controls are provided
46 through GEFANUC's iFIX software running on a PC, which is connected to the PLC through

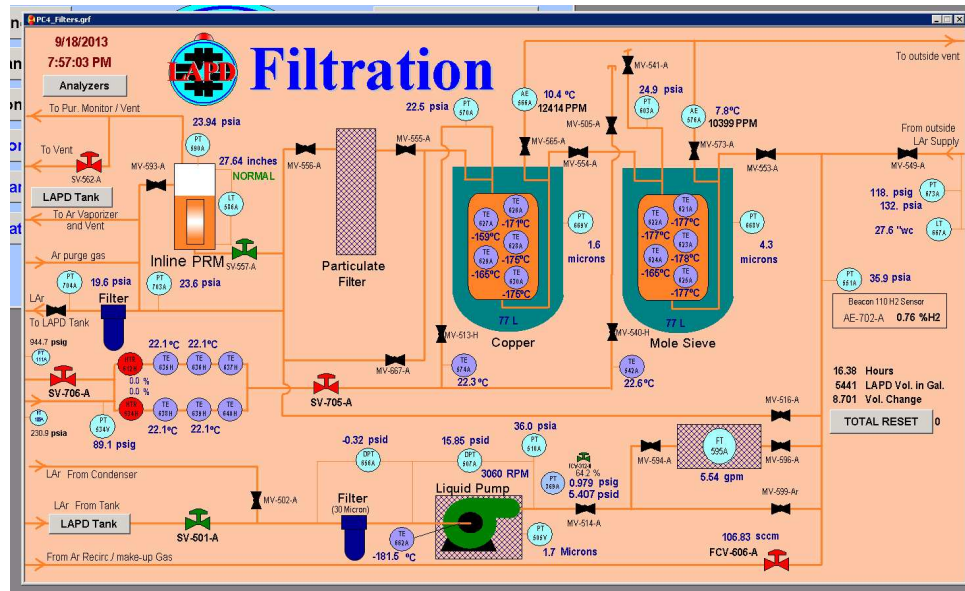


Figure 7. An example of iFIX graphical user interface for the LAPD controls.

1 local ethernet. The iFIX software allows entry of temperature and pressure set points and
 2 other operational parameters, handles alarming and remote operator controls such as opening
 3 and closing valves, displays real-time instrument values, and archives instrument values for
 4 historical viewing. An example of the iFIX graphical user interface used in the LAPD is shown
 5 in Figure 7.

6 4. Cryostat Instrumentation

7 4.1. RTD Translators

8 Two sets of three resistive thermal devices (RTDs) on translators were deployed to measure
 9 thermal gradients in the cryostat at all stages of operation and argon fill level (**why care about**
 10 **gradients?**). The motivation for installing these translators is to verify finite element analysis
 11 (FEA) calculations [22] used to model LAr mass flow in the cryostat.

12 One translator is installed near the center of the cryostat and the other is installed 1.0 m
 13 radially outward from the center. Each translator consists of a single circuit board, 50 cm long
 14 with RTDs mounted at 22.9 cm intervals for a total of 3 RTDs per circuit board as seen in
 15 Figure 9. Figure 8 shows the locations of the RTD translators inside the cryostat as well as the
 16 purity monitors, discussed in Section 4.2. The circuit board is suspended at one end of a chain,
 17 with a counter-weight at the other end of the chain to prevent movement during an electrical
 18 outage. The chains engage a 15.13 cm circumference gear that is driven externally, through a
 19 ferromagnetic seal, by an Automation Direct STP-MTRH-23079 stepper motor. The housing
 20 around the gear also includes electrical limit switches to stop the motor when the chain limits
 21 are reached. The stepper motor is controlled by an Automation Direct STP-DRV-4850 stepper
 22 drive. During a typical acquisition, the circuit board translates vertically through the cryostat
 23 with stops at predefined locations to take temperature measurements.

24 Teflon ribbon cables connect the circuit boards to a LakeShore model 218 temperature monitor
 25 which reads out all six RTDs. The stepper motor controller and LakeShore are controlled and

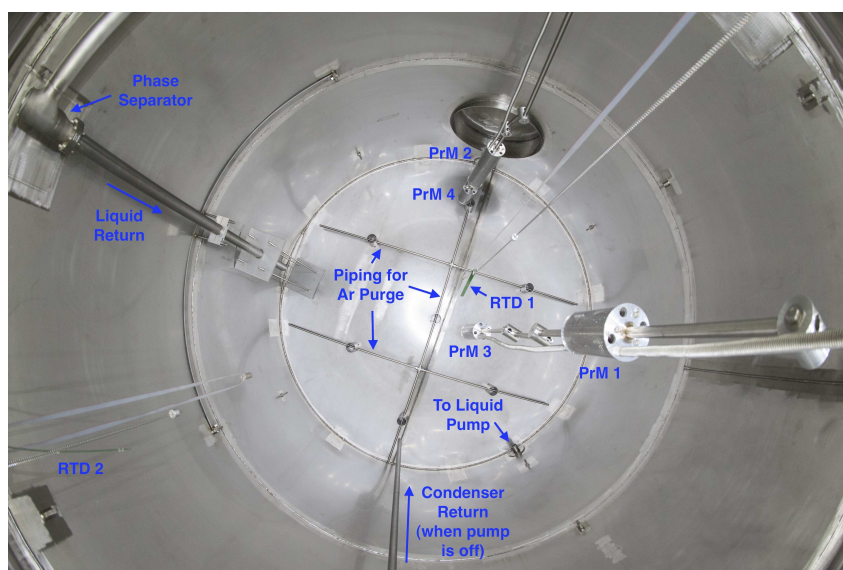


Figure 8. A photograph of the interior of the cryostat viewed from the top. The purity monitors, RTD translators and piping are shown.

1 read out by a custom LabVIEW application. The RTDs are platinum, type K 100 Ohm and were
 2 measured to be accurate to within 0.5 K. Temperature data are acquired at twenty equidistant
 3 steps throughout the height of the tank. Each data point consists of sixty-four single RTD
 4 measurements with times between steps being long enough to mitigate bias in movement and
 5 ensure thermal equilibrium. For measurements in the liquid (gas), acquisition times between
 6 data points are approximately 5 (30) minutes.

7 The liquid argon in the LAPD cryostat is not at thermal equilibrium. The vapor is continually
 8 being removed and condensed in an external condenser, then admixed with liquid argon drawn
 9 directly from the cryostat and then sent through purification filters before being returned to
 10 the cryostat. This evaporation of liquid argon from the surface is seen visually by a surface
 11 turbulence, and detected by the RTDs as a temperature drop both from the bulk liquid below
 12 the surface, and the vapor above in the ullage.

13 Figure 10 shows a scan of the cryostat taken after the first fill of LAr for the central and pe-
 14 ripheral RTD translators. Of primary note is the very sharp temperature gradient (80K/50cm)
 15 in the ullage just above the liquid surface. The top of the LAr surface was 2.9 m (115") below
 16 this point at the date of this particular run. The data shown were taken only from the downward
 17 direction of the total run, to avoid the thermal lag one sees when the circuit board is moving
 18 out of the liquid. The wait-after-move time was 5 minutes in this case.

19 Figure 11 shows a relatively quick scan with the cryostat full and the wait-after-move time
 20 of 3 minutes. It should be noted that the lowest RTD of this Spooler is located just slightly
 21 above the LAr level, even with the circuit board at the top of the limit switch. However the
 22 lower tip of the circuit board is just dipping or very near the liquid surface. As a result of the
 23 heat conduction in the circuit board, this lower RTD temperature is biased lower than it would
 24 actually be if the circuit board tip were not there. As the circuit board is lowered into the LAr,
 25 one can see the temperature dip 0.4K below the temperature of the bulk liquid. This is just the
 26 evaporative cooling of the surface layer of the LAr. Once the RTDs penetrate this surface layer,



Figure 9. A photograph of the peripheral RTD translator inside the LAPD cryostat.

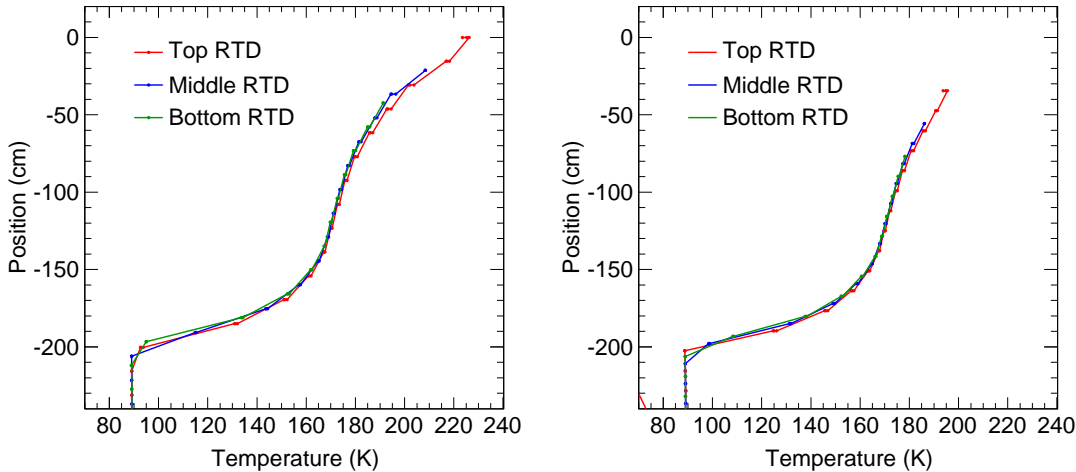


Figure 10. The cryostat temperature as measured by the three central (left) and the three peripheral (right) RTDs. Data were taken after the first trailer of liquid argon was delivered to the cryostat, corresponding to a liquid argon height of 69 cm from the bottom. On these Figures, this corresponds to a value of **200 cm** as measured from the top of the cryostat.

1 the temperature recovers to almost a constant value. Its temperature scale should be noted here.
 2 The slight change of temperature with depth is less than approximately 25mK over 2m. At the
 3 bottom of the scan there is another dip of 30mK. The returning purified LAr is introduced
 4 at the bottom of the cryostat and may be the cause of this slight dip. Looking at the spread
 5 in measurements of any one RTD at a fixed position in the liquid, the peak-to-peak spread is
 6 10mK, implying the relative precision of a single measurement is on the order of a few mK.
 7 There is a nominal agreement between our measurements and FEA calculations ([22]).

8 4.2. Purity Monitors

9 The purity of liquid argon is continuously monitored by a double gridded ion chamber im-
 10 mersed in the liquid argon volume. The fraction of electrons generated at the cathode that
 11 arrive at the anode (Q_a/Q_c) after the electron drift time, t is a measure of the electronegative
 12 impurity concentration and can also be interpreted as the electron lifetime, τ such that

$$13 \quad Q_a/Q_c = e^{-t/\tau}. \quad (1)$$

14 4.2.1. Hardware

15 The purity monitor is based on the design described in Reference [20]. It consists of four
 16 parallel, circular electrodes: a disk supporting a photocathode, two open wire grids, one anode
 17 and one cathode, and an anode disk. The anode disk and photocathode support disk are made
 18 of stainless steel; the two grid support rings are made of G-10 circuit board material with the
 19 grid wires soldered to the copper clad surface. The region in between the anode grid and cathode
 20 grid contains a series of field-shaping stainless steel rings. The two grids, each with a single set
 21 of parallel wires, are made of electro-formed gold-sheathed tungsten (AuW) with a 2.0 mm wire
 22 spacing, 25 μm wire diameter and 98.8% geometrical transparency (see Table 2).

23 The cathode grid is at ground potential. The cathode, anode grid, and anode are electrically
 24 accessible via modified vacuum grade high voltage feed-throughs. The anode grid and the field-

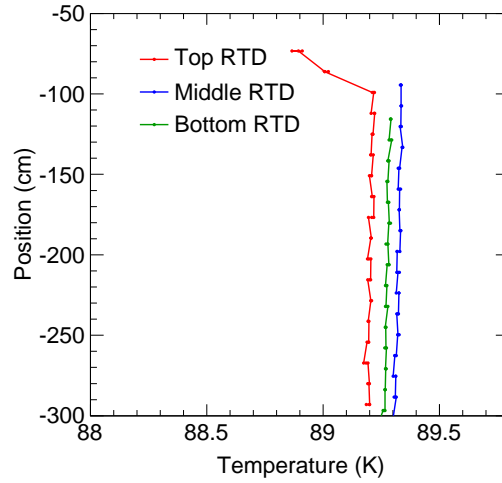


Figure 11. The temperature as measured by the three central RTDs when submerged in liquid argon. This figure illustrates the precision with which the temperature is measured. **What are the points at the top?**

1 shaping rings are connected to the cathode grid by an internal chain of 50 M Ω resistors to ensure
 2 the uniformity of the electric fields in the drift regions. The field ratios typically satisfy

$$3 \quad E_{Anode\ Grid-Anode} > 2E_{Anode\ Grid-Cathode\ Grid} > 4E_{Cathode\ Grid-Cathode} \quad (2)$$

4 to ensure maximum transparency [21].

5 The photocathode is a 1'' \times 1.5'' \times 0.03125'' aluminum slide, coated with 50 \AA of titanium and
 6 1000 \AA of gold and attached to the cathode disk [15]. A xenon flash lamp [16] is used as the
 7 light source. The UV output of the lamp has a wide spectrum above approximately 225 nm.
 8 An inductive pickup coil on the power leads of the lamp provides a trigger signal when the lamp
 9 flashes. Light is directed via three single-mode quartz optical fibers [17] to the photocathode.
 10 Only one fiber is needed the other two are for redundancy. The fibers have a 0.6 mm core
 11 diameter and 25.4 degrees of full acceptance cone. The attenuation is 0.95 dB/m at 200 nm.
 12 The fibers underwent a series of tests using a photodiode read out by an oscilloscope to measure
 13 the stability and light output linearity as a function of input light intensity and showed no
 14 anomalous behavior.

15 The electrons liberated from the photocathode drift towards the cathode grid and induce a
 16 current on the cathode. After crossing the cathode grid, the electrons drift between the two
 17 grids. During this time essentially no current is induced on the cathode or anode due to the
 18 shielding effect of the grids. After crossing the anode grid, the electrons induce a current on
 19 the anode. The signals induced on the cathode and anode are fed into two charge amplifiers in
 20 a purity monitor electronics module. The charge amplifiers have a 5 pF integration capacitor
 21 with a 22 M Ω resistor in parallel with the capacitor. The signal and high voltage are carried on
 22 the same cable and decoupled inside the purity monitor electronics module. Figure 12 shows a
 23 schematic of the liquid argon purity monitor.

24 The LAPD system employs five purity monitor units at different locations. Each purity
 25 monitor is contained in a stainless steel, perforated Faraday cage to isolate the system from the

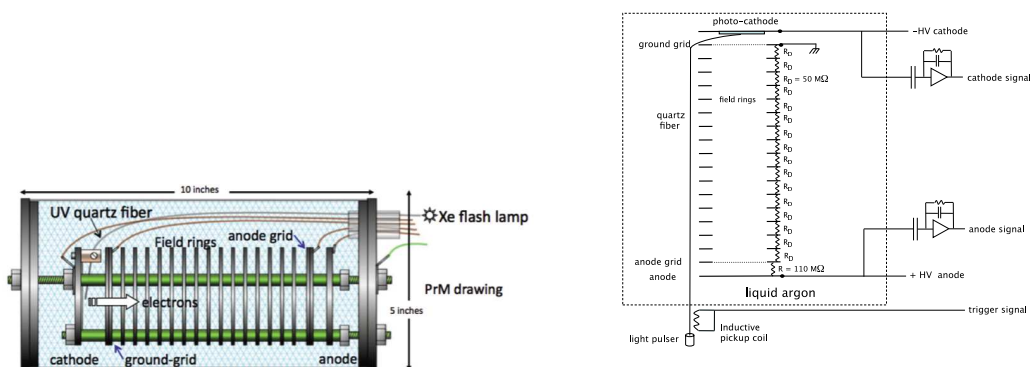


Figure 12. Drawing and schematic of a Liquid Argon Purity Monitor employed in LAPD.

1 outside electrostatic interference. There are two types of purity monitors with different lengths
 2 and different numbers of field-shaping rings: three long purity monitors that are 55 cm and
 3 two short purity monitors that are 24 cm. The operational range of Q_a/Q_c for which a purity
 4 monitor can make sensible measurements is about 0.05 - 0.95. Thus, longer electron drift lengths
 5 correspond to operational ranges shifted to sample larger electron lifetimes. An assembly of one
 6 long purity monitor and one short purity monitor is located vertically along the central axis
 7 of the cryostat. Another identical assembly is located at a distance of 1.1 m away from the
 8 center of the cryostat. Figure 13 shows a photograph of the assembly located near the cryostat
 9 periphery. One long purity monitor, referred to as the inline purity monitor, is located in the
 10 circulation pipe to measure the liquid argon purity before the liquid enters the cryostat. Three
 11 flash lamps are used for the two purity monitor assemblies and the inline purity monitor. Table 2
 12 shows the geometrical characteristics and voltage settings of the purity monitors installed in the
 13 cryostat.

14 4.2.2. Data Acquisition

15 A Visual Basic program running on a Tektronix [18] digital storage oscilloscope (5054 TDS)
 16 is used for control and data acquisition for the purity monitor system. The program controls
 17 operations through the Fermilab-designed automation module, which controls the high voltage
 18 power to the purity monitor and the flash lamp operation. Measurements of the electron lifetime
 19 are taken several times a day. Each measurement takes about one minute. The flash lamp and
 20 the high voltage to the purity monitors are only powered during this time to protect the flash
 21 lamp, minimize degradation of the quartz fiber and reduce dust/particle accumulation on the
 22 purity monitor photocathode. The automation module will switch off both the flash lamp power
 23 supply and high voltage to the purity monitor if the lamp has been flashing for more than 140
 24 seconds. An 8-channel analog multiplexing unit (MUX) is used to select which purity monitor
 25 signal is readout. Each channel of the MUX has four inputs, three of which read the cathode
 26 and anode signals from one purity monitor after the amplifiers and the trigger signal from the
 27 inductive pickup coil. Figure 14 shows a block diagram of LAPD purity monitor system.

28 The program initializes and reads out the signals from each purity monitor one by one. When
 29 the flashlamp fires, a large noise signal is induced on the cathode and anode connections which
 30 distorts the shape of the electron signals. This noise signal is measured and recorded before



Figure 13. One assembly of one long purity monitor and one short purity monitor inside LAPD.

Table 2
Geometrical characteristics and voltage settings of the purity monitor.

	Long monitor	Short monitor
Cathode, Anode disk, grid diameter	8 cm	
Cathode-Anode total drift distance	50 cm	19 cm
Cathode grid to Anode grid distance	47 cm	16 cm
Cathode-Cathode Grid gap	1.8 cm	
Anode Grid-Anode gap	0.79 cm	
Number of field-shaping rings	45	15
Number of resistors	46	16
Anode disk/Cathode disk thickness	0.23 cm	
Anode grid/Cathode grid thickness	0.24 cm	
Field-shaping ring thickness	0.23 cm	
Gap between rings	0.79 cm	
Nominal Cathode Voltage	-100 V	-100 V
Nominal Anode Voltage	5 kV	2 kV
$V_{Anode\ Grid}/V_{Anode}$	0.948	0.865
Nominal $E_{Cathode\ Grid-Cathode}$	56 V/cm	56 V/cm
Nominal $E_{Cathode\ Grid-Anode\ Grid}$	101 V/cm	108 V/cm
Nominal $E_{Anode\ Grid-Anode}$	329 V/cm	342 V/cm

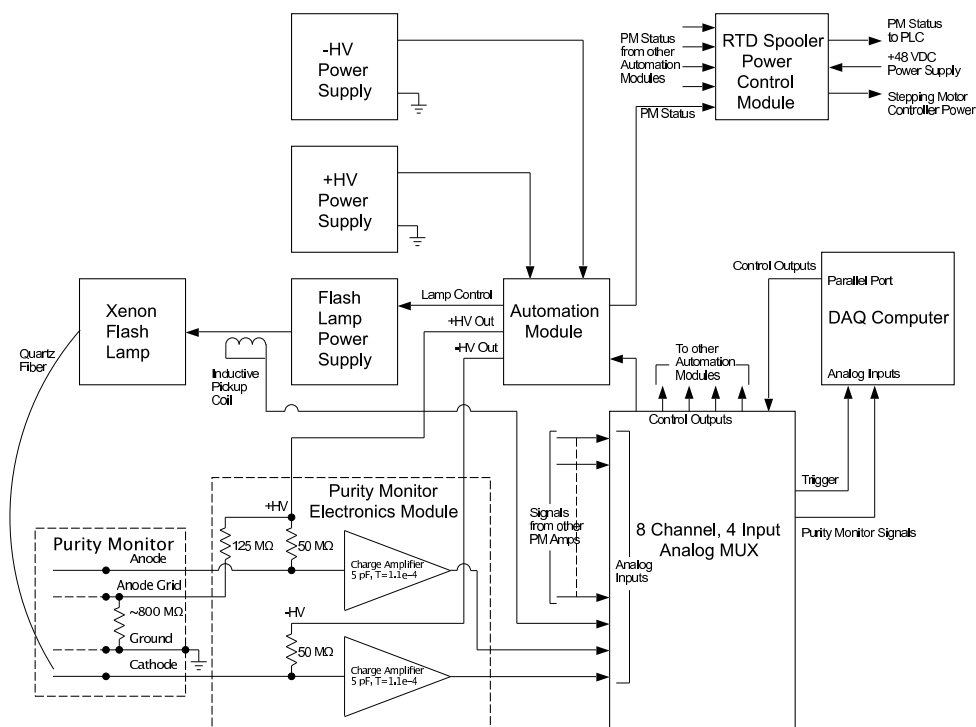


Figure 14. Block diagram of LAPD purity monitor system.

1 turning on the high voltage to the purity monitors. The anode and cathode signals from each
 2 purity monitor are then measured by constructing the average of ten waveform samples per
 3 acquisition which are then stored for offline analysis. A plot of the averaged and smoothed
 4 signal traces produced from the digitizer card, before and after noise subtraction, is shown in
 5 Figure 15.

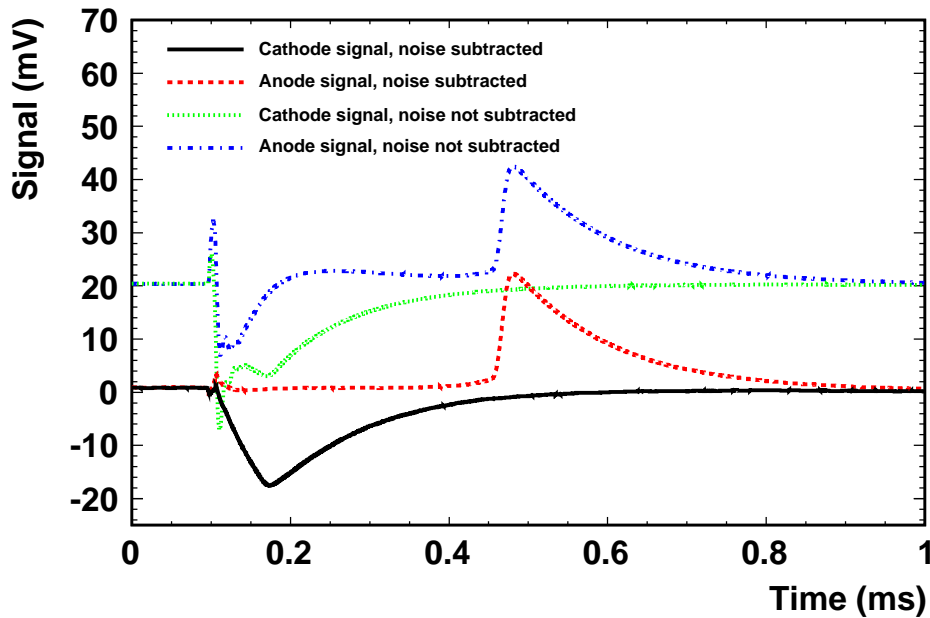


Figure 15. A screenshot of anode and cathode signals before and after noise removal from the digitizer.

6 During the course of the project, the Tektronix-based purity monitor DAQ system was re-
 7 placed by a digitizer PC equipped with a 12-bit AlazarTech ATS310 card capable of sampling
 8 at 20 MHz. The new DAQ system performed as well as the oscilloscope and was procured at
 9 a lower cost. The original Visual Basic purity monitor DAQ program from the first run was
 10 modified to run with the digitizer utilizing the development kit for the ATS310. The sampling
 11 rates were 2 MHz (5 MHz) for the long (short) purity monitors. The range of voltages used for
 12 both long and short purity monitors was ± 50 mV.

13 An additional source of electrical noise that affected the operation of the purity monitor DAQ
 14 was found to be the RTD translator stepper motor controllers. These controllers have a DC
 15 to DC switching converter that provides the holding current to the stepper motors used in the
 16 RTD translator system. The most effective way to mitigate this noise source was to remove
 17 the 48 volt DC bulk power to the stepping motor controllers whenever the purity monitor DAQ
 18 was running. After the purity monitors were turned off by the DAQ, the 48 volt DC power was
 19 restored to the stepping motor controllers and a reset signal was given to the controllers so that
 20 they would reindex back to the zero starting point for their data collection.

4.2.3. Systematic Uncertainties

There are several systematic effects which need to be accounted for to make a reliable measurement of argon purity. The lifetime relies on measurements of V_a and V_c , which in turn depend on amplification of induced currents on the anode and cathode. The potential exists for differences in amplification between the anode and cathode signal voltages to have an impact on the lifetime. We model the amplification as $V_a = g^\alpha Q_a$ and $V_c = g^\beta Q_c$, where g^α and g^β are constants. If the two amplifiers used for the anode and cathode signals are switched, the amplification becomes $V'_a = g^\beta Q_a$ and $V'_c = g^\alpha Q_c$. The primes indicate measurements taken with the amplifiers for the anode and cathode swapped. The lifetime and attenuation calculations can then be calibrated by making measurements of V_a , V'_a , V_c , and V'_c using

$$\frac{g^\alpha}{g^\beta} = \sqrt{\frac{V_a/V_c}{V'_a/V'_c}}. \quad (3)$$

During a span of several days at nearly constant argon purity, measurements were taken with the amplifiers swapped to measure the ratio g^α/g^β . With the measurements taken, a correction to the lifetimes was applied using

$$\tau = \frac{t}{\ln((Q_c/Q_a) \times (g^\alpha/g^\beta))}. \quad (4)$$

Another systematic uncertainty examined is the effect of the values of the high voltages applied to the cathode and anode. To examine this effect, the high voltages applied to the anode and cathode were varied and many measurements were taken during a span of a few hours. A short purity monitor was run with high voltages on the anode at 2 kV, 3 kV, 4 kV, and 5 kV. Both studies resulted in purity measurements consistent with those at nominal high voltage.

4.3. Gas Analyzers

4.3.1. Oxygen, Water and Nitrogen Monitors

LAPD has an extensive gas analysis system to monitor and diagnose the processes that take the cryostat from atmospheric air to ultra pure liquid argon. The system consists of seven commercial gas analyzers. Four of these analyzers measure the oxygen concentration and together they span the range from 0.1 ppb to 5000 ppm. These four oxygen analyzers are augmented by two 0.1-25% oxygen sensors which monitor the purge of the cryostat of air and are described in Sec. 4.3.2. Two of these seven gas analyzers measure the water concentration and these span the range from 0.2 ppb to 20 ppm. Dew point meters installed in series with these water analyzers extend the measurement range from 20 ppm up to ambient dew points as high as 20,000 ppm water. A nitrogen analyzer completes the array of seven gas analyzers with a range that spans 0.1 to 100 ppm.

The gas analyzers are fed by a local switchyard of 56 diaphragm valves. These valves direct the gas flow from five primary locations in the system to the seven gas analyzers. In addition to the five primary locations, argon and nitrogen gas from utility sources are available to supply analyzers when measurement from a system location is not required. A primary location or utility gas can feed anywhere between none and all of the gas analyzers. The primary measurement locations are the liquid argon cryostat, with the option of sampling from either the gas or liquid phases, pump discharge, molecular sieve filter output, oxygen filter output, and the liquid argon fill connection. An oil free vacuum pump is also part of the switchyard and can evacuate the tubing that connects the measurement locations and the gas analyzers. Evacuation of the sample lines when switching sample locations greatly reduces the time required to reach equilibrium when the measured contamination is at the parts per billion concentration. A high purity metal

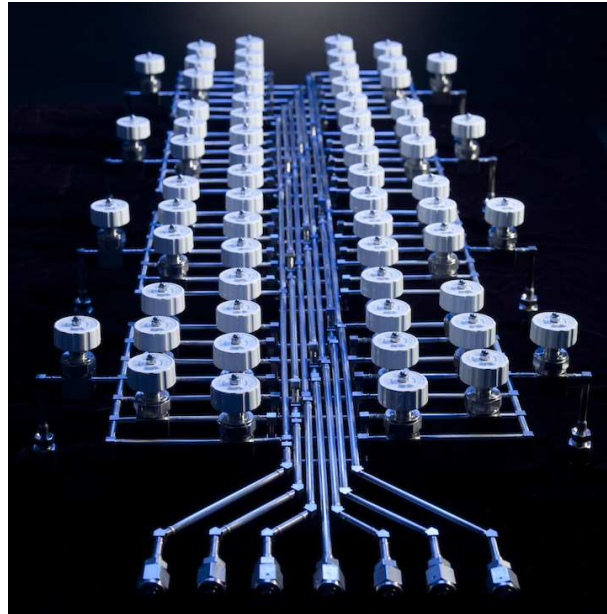


Figure 16. Gas distribution switchyard - liquid argon gas sampling master distribution panel.

1 bellows pump boosts the sample pressure from the 2 psig operating pressure of the liquid argon
2 cryostat to the 15-20 psig inlet pressure required by the gas analyzers. A photograph of the gas
3 distribution switchyard is shown in Figure 16.

4 Filter output sampling allows determination of filter performance and capacity. Sampling the
5 liquid argon fill connection is critical to ensure that the liquid argon supply is within specification.
6 For example, a trailer of liquid argon was rejected because it was so far out of specification it
7 would have required an impractical number of filter regenerations to process. Without this
8 extensive gas analyzer system it would be very difficult to successfully take the cryostat from
9 ambient air to ultra pure liquid argon.

10 4.3.2. Oxygen Capillary Detectors

11 We deployed 13 industrial type (Citicell model 2FO) oxygen sensors, configured in two strings
12 of 6(7) each consisting of capillary tubes placed at different heights, to measure the oxygen
13 concentration during the initial gaseous argon purge. One string was placed near the cryostat
14 wall and the other was placed near the cryostat center. The end of each tube is vertically spaced
15 30" from the next in the string, with the string spanning the height of the cryostat. The central
16 set was placed on the tank axis, the peripheral set was 44 inches radially out. The sampling tube
17 inlets were spaced 30 inches apart, spanning the height of the tank. The sensors are inside glass
18 "jam jars" with plastic coated lids. The sample tubes are 0.063 inch diameter capillaries, and
19 run continuously from the intake point through a CF flange to the jars. All capillaries are the
20 same length, with the excess length coiled up above the feed-through flange, to assure matched
21 time response. The jars are mounted on feed-through flanges.

5. Results from Operation Modes

The LAPD was operated in two separate run periods. In each period, the cryostat was operated in three phases; a gaseous argon purge, gaseous argon recirculation, and liquid recirculation. The first run period was September 2011 to April 2012. Each of the three phases of operation were performed to test the devices and filters. For this period, the cryostat was filled 1/3 full to confirm the feasibility of measuring the liquid argon purity.

The second period was from December 2012 through October 2013. For each period, we performed a single argon purge at the beginning of the period, followed by a single phase of gaseous argon recirculation. The cryostat was then filled with liquid argon and measurements of the liquid argon purity were performed under various operating conditions. This section describes the results for the second period, and when applicable, measurements are compared to those obtained in the first run period.

5.1. Gaseous Argon Purge

A gaseous argon purge was performed at the beginning of each run period. In this phase of operation, gaseous argon is pumped from the bottom of the cryostat displacing the ambient air which exits out the room temperature feedthroughs at the top of the cryostat. This method mimicks an argon “piston” in the sense that the higher density gaseous argon engenders a boundary between it and the ambient air, which moves vertically upwards. For the first period, the two sets of sampling gas capillaries, described in Section 4.3.2, were installed to measure the oxygen concentration and follow the rise of the argon gas as it displaces the lighter room air.

The purpose of these measurements was to understand the average gas purity and obtain information for comparison to FEA flow models to validate or improve those models. The spatial and temporal concentration measurements provide information about the degree of diffusion and mixing during purges. Each purge lasted approximately 8 volume exchanges (~ 24 hours) and corresponds to a 3.8 ft/hour piston rise rate and 2.9 (3.4) hours per volume exchange for the first (second) period. The gaseous argon flow rate was constant throughout each purge. Figure 17 shows the fraction of ambient air retained with respect to the measured oxygen levels during the gaseous argon purge in the first run period for the seven capillary tubes installed in the central region of the cryostat and the six capillary tubes installed in the peripheral region of the cryostat. The front of gaseous argon is clearly present as indicated by the successive reduction of air seen by each capillary tube as a function of time.

At the end of the first period purge, the capillaries were removed. The removal lasted 15 minutes, during which time argon gas flowed into the cryostat at 5-6 SCFM. During the extraction, the water, oxygen, and nitrogen monitors were switched to argon gas utility as a precaution because the bellows pump drawing gas from the cryostat could pull a vacuum on the cryostat if the argon flow into the cryostat stopped. After these devices were switched back to measuring the cryostat gas, an increase of about 0.2 ppm O₂ and 0.4 ppm N₂ was observed. With the capillaries removed, the makeup gas flow dropped from 0.35 SCFM to 0.15 SCFM. At the end of the purge, 7158 ft³ had passed through the cryostat, corresponding to 8.2 volume exchanges. The oxygen level was reduced to 5.2 ppm, the water concentration was reduced to 996 ppb, and the nitrogen concentration was reduced to 13.4 ppm. Figure 18 shows the concentrations of water and oxygen during the gaseous argon purges for both periods, along with the results from the capillary tube oxygen measurements from the first period. In both run periods the water concentration was reduced to approximately 1 ppm. The oxygen concentrations were reduced to 10(7) ppm for the first (second) run period. Throughout both purges, the nitrogen concentration remained nominally stable at 18 ppm. The argon purges for both run periods delivered similar results.

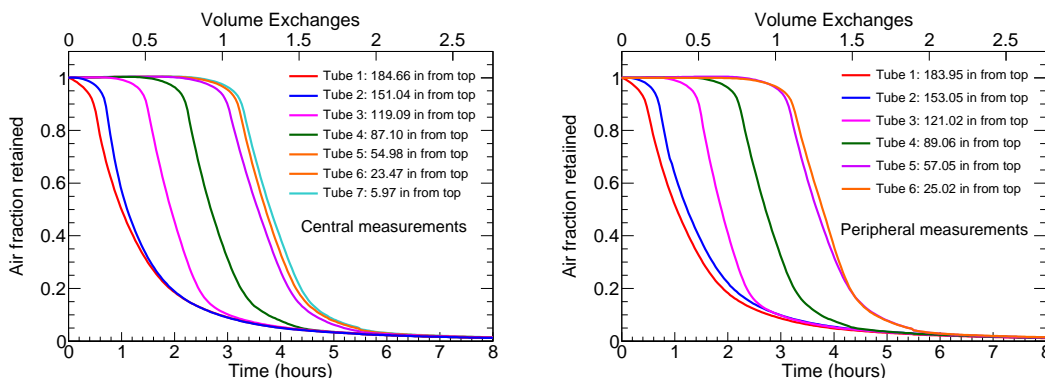


Figure 17. Oxygen concentrations for the a) central and b) peripheral gas sampling capillaries taken at several heights with respect to the cryostat bottom obtained during the initial gaseous argon purge for the first run period. **SHOW THE FEA CALCULATION TOO!**

5.2. Gas Recirculation

After the removal of the ambient air from the argon purge, argon gas was pumped through the molecular sieve and oxygen filter at a rate of a volume exchange every 3.4 hours, then returned to the cryostat. The gas recirculation for the second period ran for about 77 volume exchanges corresponding to one week. Figure 19 shows the oxygen and water concentrations, measured by the water and oxygen gas analyzers, for the gas recirculation phase. At the end of this phase, the oxygen concentration was reduced to approximately 20 ppb and the water concentration reached a stable value of 667 ppb. The nitrogen concentration was reduced to 13.7 ppm. A gap in the data between 27 and 37 volume exchanges corresponds to a time during which the gas analyzers were sampling alternate components of the system. The overall results for the gas recirculation phase indicate that water outgasses from all surfaces of the cryostat and piping, and that the outgassing rate eventually matches the filtration rate.

5.3. Liquid Argon Filling

For the first period, the cryostat was only filled to 1/3 capacity, which ended prematurely due to a power outage. For the second period, the cryostat was filled with LAr from the **D0** calorimeter at Fermilab. The duration of each fill varied from 4 to 6 hours. Table 3 presents the LAr trailer contaminant concentrations along with details of each successive fill for the second run period. The four trailers were delivered over a period of two weeks in January, 2013. The total volume of LAr placed in the cryostat was 5630 gallons, corresponding to 29.7 tons.

5.4. Liquid Argon Recirculation

After the cryostat was full, the liquid recirculation pump was started at a rate of 9.4 GPM. Filtration proceeded by routing liquid argon through the **two filters**. We had several opportunities to determine the performance of the filters and their capability to reduce the impurities, at various times throughout operation. Figure 20 shows the water and oxygen concentrations in the cryostat liquid as measured by the **HaloTrace and Nanotrace** as a function of time, for three select intervals immediately preceding purity monitor operation. The measured oxygen concentration was compared to simulation assuming perfect mixing in the cryostat (**Need explanation**

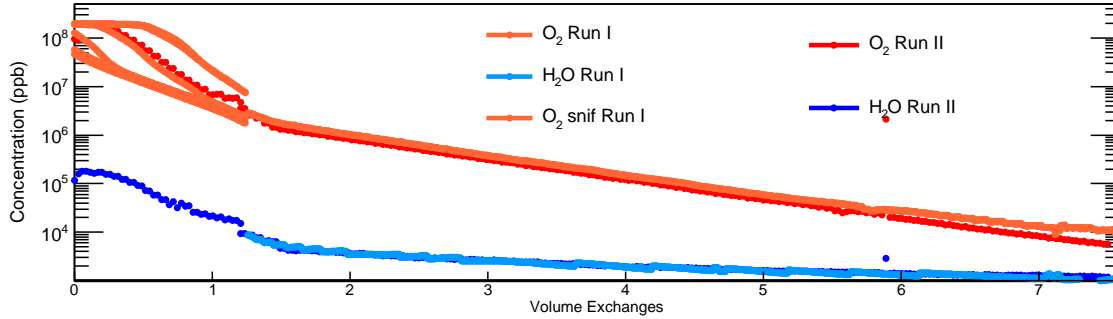


Figure 18. The water and oxygen concentrations in the LAPD during the two gaseous argon purges as a function of the number of volume exchanges. The plot shows the water concentration and the oxygen concentration measured by both the gas analyzer and the oxygen capillary tubes. Similar results were obtained for both purges.

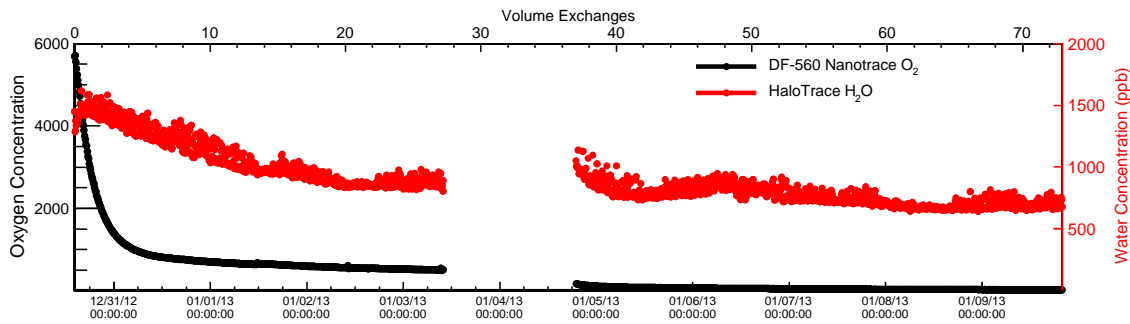


Figure 19. The water and oxygen concentrations in the cryostat gas during the gas recirculation phase of the second period, plotted as a function of time and of the number of volume exchanges.

	O_2 (ppb)	H_2O (ppb)	N_2 (ppm)	LAr height (inches)	GPF	Rate (GPM)	Net gallons
Trailer 1	202	99	10	27	1325	≈ 500	1325
Trailer 2	200	225	9	58	2832	587	1507
Trailer 3	400	180	9	87	4259	520	1427
Trailer 4	197	66	10	115	5630	400-525	1371

Table 3

Concentrations of oxygen, water, and nitrogen measured in each trailer before introduction into LAPD. The LAr height is measured in inches from the bottom of the cryostat corresponding to the number of gallons delivered to the cryostat in each fill (GPF). Also shown is the rate in gallons per minute (GPM).

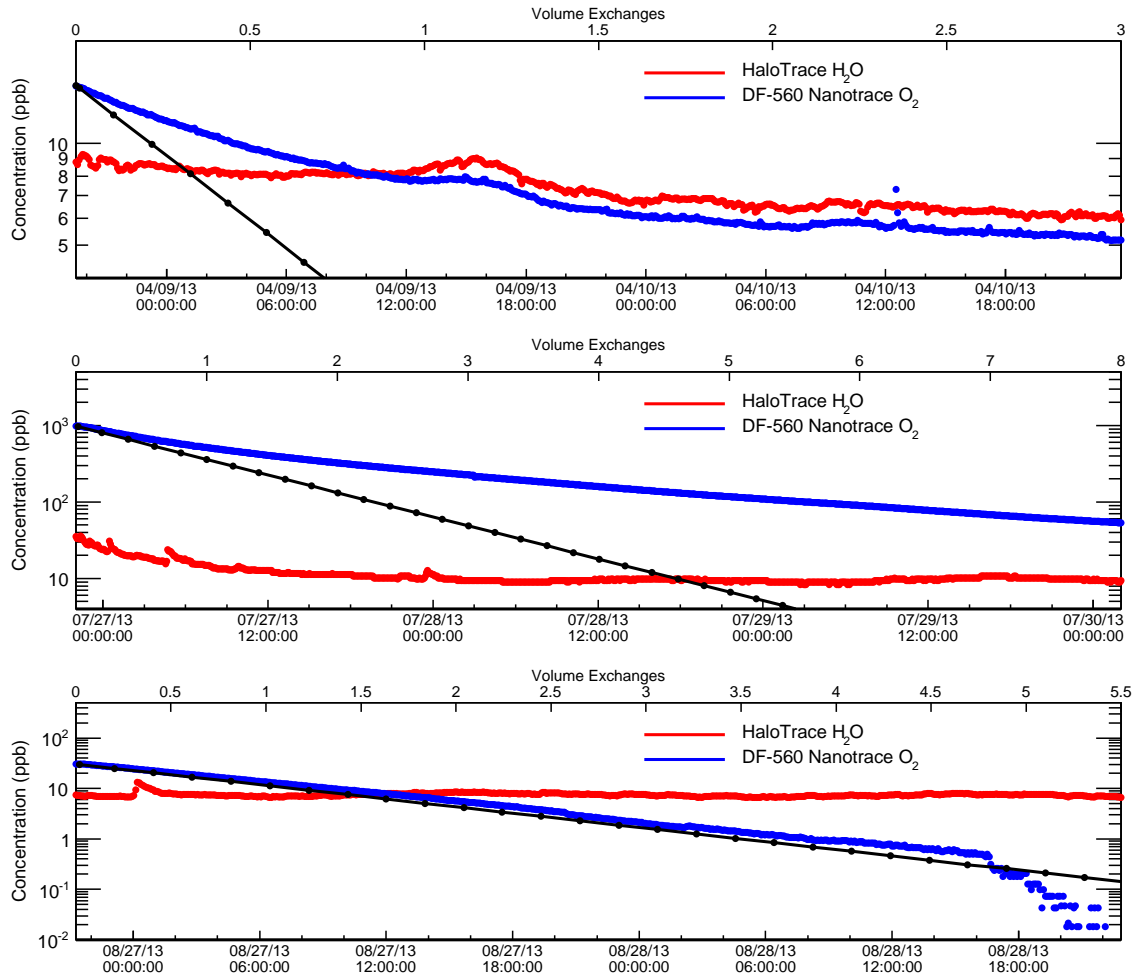


Figure 20. The water and oxygen concentrations in the cryostat liquid for three time intervals before purity monitor operation. The measured oxygen concentration (blue line) is compared to a simulation assuming perfect mixing (black line).

1 for “perfect mixing”). The figure shows that in the first two time intervals, perfect mixing was
 2 not achieved. This suggests that what?. However, in the last time interval, perfect mixing was
 3 nearly achieved.

4 Figure 21 shows the water and oxygen concentrations measured in the cryostat vapor space
 5 with the cryostat totally filled with LAr, along with the temperature in the LAPD hall. The
 6 temperature and the water concentration in the cryostat vapor space are closely correlated and
 7 suggests significant outgassing of water in this region.

8 After several liquid volume exchanges, the contamination was sufficiently low to begin opera-
 9 tion of the four purity monitors inside the cryostat and the inline purity monitor upstream from
 10 the filters. The signal attenuation is defined as $1 - Q_a/Q_c$, where Q_a and Q_c are the anode and
 11 cathode peak pulse heights, respectively. Figure 22 shows the cathode peak pulse height and the
 12 attenuation over the complete LAPD run with several periods of extended stable running with

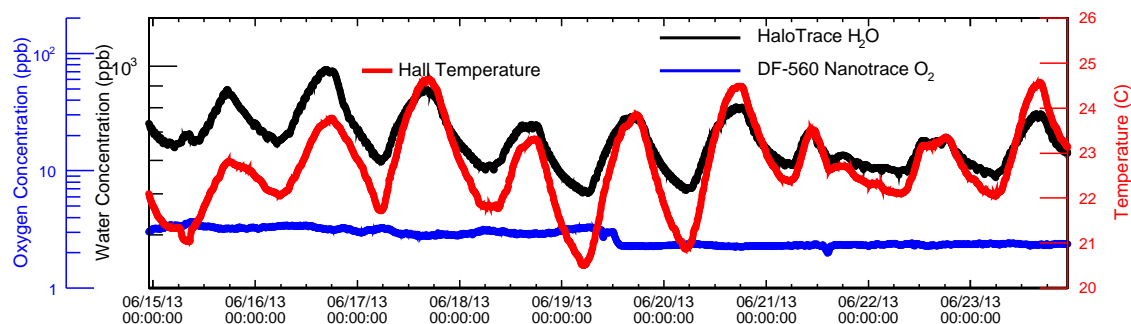


Figure 21. The water and oxygen concentrations measured in the cryostat vapor space with the cryostat totally filled with LAr. Also shown is the temperature in the LAPD hall for the same time period.

1 measured lifetimes of more than 3 ms and occasionally more than 6 ms. The cathode signal ap-
 2 pears to become less efficient over time. Nevertheless, even with low cathode signals, measured
 3 lifetime values are consistent with times during which good signals were achieved. The pump
 4 speed, and thus the volume exchange rate were changed over several time intervals throughout
 5 the run and found no correlation between volume exchange rate and measured lifetime values.

6 6. Discussion and Conclusion

7 **This needs some work.** The primary goal of the Liquid Argon Purity Demonstrator (LAPD)
 8 has been achieved. The required level of purity can be achieved in a large volume of liquid argon
 9 without first evacuating the vessel containing the liquid and LArTPC. This test is motivated by
 10 the desire to obviate costs associated with the construction of an evacuable cryostat for future
 11 multi-kiloton detectors.

12 In addition to showing that evacuation is not necessary for achieving long electron lifetimes,
 13 we studied temperature gradients, liquid argon volume exchanges, filter capacity, and the effect
 14 of other materials. **Discuss each of these.** The results demonstrated that the technique works
 15 in the presence of material and nominal electron drift lifetimes were recovered after **X** volume
 16 exchanges.

17 Indications from the MTS suggest the water concentration increases as the sample temperature
 18 increases, and the electron lifetime decreases. This demonstrates two major findings from the
 19 MTS. First, there is a direct relationship between electron lifetime and water concentration.
 20 Second, the water concentration does not change when materials are submerged in the liquid,
 21 but it does increase when materials are in the vapor space.

22 Acknowledgments

23
 24 We thank the staff at FNAL for their technical assistance in running the LAPD experiment. We
 25 acknowledge support by the Grants Agencies of the DOE.

26 REFERENCES

27 1. J. N. Marx and D. R. Nygren, Phys. Today **31N10**, 46 (1978).

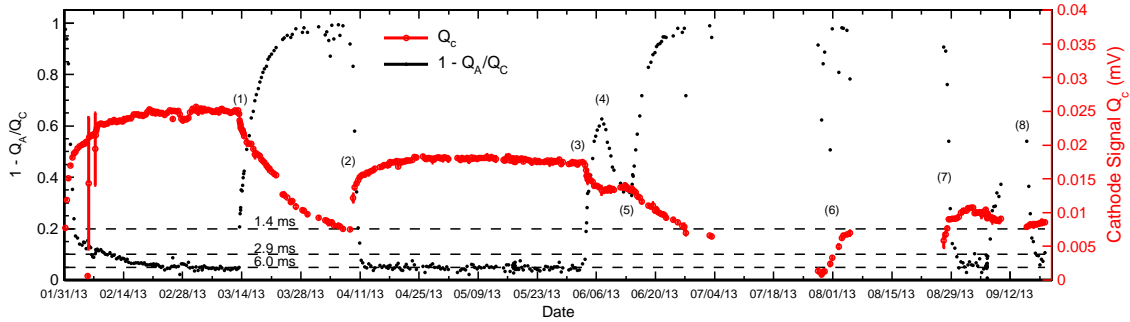


Figure 22. The cathode signal (Q_c) indicated as open red circles and the attenuation ($1 - Q_A/Q_C$) indicated as solid black circles for recirculated liquid argon over all LAPD running. The attenuation is correlated with electron lifetime, calculated at attenuations of 0.05, 0.1, and 0.2. Gaps in the data occur when either the purity monitors do not have sufficient resolving power or when they were not operating. Special events are enumerated with the following descriptions: (1) Circulation pump trip for an extended time period. (2) Beginning of containment cleanup (see Figure 20 (top)). (3) Pump trip lasting one hour resulting in subsequent zero flow to the filters (4) Start of flow to filters after the pump trip. (5) Stopped pump for removal and repair (6) Start of second cleanup (see Figure 20 (middle)). (7) Start of third cleanup (see Figure 20 (bottom)). (8) Pump restart after a few-day period to insert a digital camera.

- 1 2. E. Gatti *et al.*, IEEE Trans. Nucl. Sci. **26**, 2910 (1979).
- 2 3. T. Akiri *et al.* (LBNE Collaboration), arXiv:1110.6249 [hep-ex].
- 3 4. S. Amerio *et al.* (ICARUS Collaboration), Nucl. Instrum. Meth. A **527**, 329 (2004).
- 4 5. C. Rubbia, *et al.* (ICARUS Collaboration), Journal of Instrumentation, **6** P07011 (2011).
- 5 6. R. Andrews, W. Jaskierny, H. Jostlein, C. Kendziora, S. Pordes and T. Tope, Nucl. Instrum. Meth. A **608**, 251 (2009).
- 6 7. W. Jaskierny, H. Jostlein, S. H. Pordes, P. A. Rapidis and T. Tope, FERMILAB-TM-2384-E.
- 7 8. C. Anderson, *et al.* (ArgoNeuT Collaboration), Journal of Instrumentation, **7**, P10019 (2012).
- 8 9. A. Ereditato, *et al.*, Journal of Instrumentation, **8**, P7002 (2013).
- 9 10. Sigma-Aldrich, P.O. Box 14508, St. Louis, MO 63178 USA.
- 10 11. BASF Corp., 100 Park Avenue, Florham Park, NJ 07932 USA.
- 11 12. Aspen Aerogels, Inc., 30 Forbes Road, Building B, Northborough, MA 01532 USA.
- 12 13. Barber-Nichols Inc., 6325 West 55th Avenue, Arvada, CO 80002 USA.
- 13 14. Micro Motion, Inc., 7070 Winchester Circle, Boulder, CO 80301 USA.
- 14 15. Platypus Technologies, LLC, Madison, WI USA.
- 15 16. Newport Corp., 1791 Deere Avenue, Irvine, CA 92606 USA.
- 16 17. Polymicro Technologies, 18019 N 25th Ave, Phoenix, AZ 85023 USA.
- 17 18. Tektronix Inc., 14200 SW Karl Braun Drive, Portland, OR 97077 USA.
- 18 19. B. Rebel, M. Adamowski, W. Jaskierny, H. Jostlein, C. Kendziora, R. Plunkett, S. Pordes and R. Schmitt, T. Tope and T. Yang, J. Phys. Conf. Ser. **308**, 012023 (2011).
- 19 20. G. Carugno, B. Dainese, F. Pietropaolo and F. Ptohos, Nucl. Instrum. Meth. A **292**, 580 (1990).
- 20 21
- 21 22
- 22 23

- 1 21. O. Bunneman, B. Cranshaw and J.A. Harvey, Can J. Res. **27**, 191 (1949)
- 2 22. E. Voirin, LAPD Cryostat Interior temperatures-RTD measurements and CFD models of
3 Liquid and Gas Temperatures, LARTPC-doc-635-v4, 5/13/2013
- 4 23. R. Schmitt, "A model for purging a 15,000 ton LARTPC tank," Presented at the Cryogenic
5 Liquid Detectors for Future Particle Physics Workshop at LNGS, (2006).